Journal of Arid Environments 110 (2014) 53–59

Contents lists available at ScienceDirect

Journal of Arid Environments

journal homepage: www.elsevier.com/locate/jaridenv

Tree-ring based evidence of the multi-decadal climatic oscillation during the past 200 years in north-central China

Shuyuan Kang [a, *], Achim Bräuning [b], Hongyuan Ge [c]

[a] Key Laboratory of Desert and Desertification, Cold and Arid Regions Environmental and Engineering Research Institute, Chinese Academy of Sciences, Lanzhou, Gansu Province, 730000, China
[b] Institute of Geography, University of Erlangen-Nürnberg, Kochstrasse 4-4, Erlangen, 91054, Germany
[c] Sidalong Protection Station of Qilian Mountain Nature Resever, Zhangye, Guansu Province, China

ARTICLE INFO

Article history:
Received 20 July 2013
Received in revised form
9 June 2014
Accepted 23 June 2014
Available online

Keywords:
Dendroclimatology
Drought events
Drought variability
Multi-decadal
North-central China
Pacific decadal oscillation

ABSTRACT

As the northern fringe of the Asian summer monsoon region, north-central China (hereafter NCC) is highly sensitive to climate change. It is important to understand drought variability and the associated mechanisms in this region since precipitation changes have direct impacts on human society in this semiarid-arid area. In this study, a new tree ring-width based drought reconstruction (AD 1804–2010) was established in the Songmingyan Nature Reserve, which lies in NCC. This reconstruction illustrates the severe drought periods occurring in the 1860s, 1928–1932 and 1991–2000, with recurring drought intervals being about 60 years. The first principal component of the five chronologies from NCC shows strongly coherent drought variability with the other single-site records and can thus be used as an indicator of regional moisture variations. Combining the Monsoon Asia Drought Atlas (hereafter MADA) dataset and the dry-wet index (hereafter DWI) dataset from eastern China, the spatial distribution of moisture variability for three selected drought events is mapped. It is found that northern China and Mongolia experienced dry conditions during the three severe drought periods, whereas wet conditions prevailed in the middle and lower reaches of the Yangtze River. The Pacific Decadal Oscillation (hereafter PDO) might have been one of the possible causes responsible for multi-decadal drought variability over NCC, with the PDO warm phases being associated with drought conditions and the cold phases corresponding to wet conditions over NCC.

1. Introduction

Moisture variations in north-central China (hereafter NCC) are predominantly influenced by the Asian summer monsoon (hereafter ASM; Chen et al., 2008). The varying intensity of the ASM activity results in the occurrence of severe drought and floods, which impact on agricultural harvest yields in NCC and the economic wellbeing of many people. Therefore, detailed understanding of the intensity of climate change and its possible physical mechanisms over the NCC region is necessary. Based on meteorological records, previous studies have demonstrated the interconnections between precipitation variability in North China and the atmospheric circulation over the Pacific Ocean (Ma, 2007). Observational composite analysis reveal that the warm Atlantic Multi-decadal Oscillation (hereafter AMO) is linked to enhanced precipitation in the north of East China and reduced precipitation in the south (Li and Gary, 2007). However, the shortness of regional instrumental records limits the understanding of long-term drought variability and its forcing mechanisms in this area. Tree-rings are one of the most important proxy indicators for studying past climatic changes (Shao et al., 2007). A number of tree-ring studies have focused on the arid western regions of China (He et al., 2013; Yang et al., 2012a, 2013a; Qin et al., 2010, 2013). Tree-ring studies conducted in NCC have revealed climate changes during recent centuries (Fang et al., 2010; Li et al., 2007; Song and Liu, 2011). However, most of these dendroclimatological studies were conducted using single-site reconstruction. Meanwhile, new techniques of tree-ring record standardization have been developed and improved the strength of the paleoclimatic information stored in tree-ring variations (Yang et al., 2012b,c).

We have investigated regional moisture variations and their possible association with the air-sea coupling system in NCC. In this

* Corresponding author. 320 Donggang West Rd., Cold and Arid Regions Environmental and Engineering Research Institute, Chinese Academy of Sciences, Lanzhou, Gansu Province, 730000, China. Tel.: +86 931 4967538; fax: +86 931 4967488.
E-mail address: kangshuyuan1982@163.com (S. Kang).

http://dx.doi.org/10.1016/j.jaridenv.2014.06.003
0140-1963/

paper we firstly introduce a new tree-ring width chronology in Songmingyan Nature Reserve (hereafter SNR) from NCC, and identify extreme drought events recorded in tree-ring variations. Secondly, we compare our chronology to other precipitation and Palmer Drought Severity Index (hereafter PDSI) reconstructions from nearby regions to investigate regional signals of moisture variability. Thirdly, we map the spatial distribution of moisture conditions during three severe drought periods (1860s, 1928–1932 and 1991–2000) recorded in the regional tree-ring chronology using the two datasets of Monsoon Asia Drought Atlas (hereafter MADA) and the dry-wet index (hereafter DWI). Finally, multi-decadal drought variability over the NCC was analyzed by correlating the tree-ring chronologies with the Pacific Decadal Oscillation (hereafter PDO).

2. Materials and methods

2.1. The SNR sampling sites and datasets

The samples were collected in the Songmingyan Nature Reserve (102°43′ E to 103°42′ E, 35°02′ N to 35°36′ N). The SNR is situated in the eastern part of the NCC, an area of marginal ASM influence. Thus, the ecological and hydrological resources are sensitive to fluctuations in intensity of the ASM. The studied tree species is spruce (*Picea asperata*), a dominant tree species growing on south-facing mountain slopes. The vegetation at the sampling site comprises species such as *Syringa oblata*, *Caragana stenophylla* and *Artemisia gmelinii*, etc.

Three meteorological stations (Lintao, Linxia and Hezuo) are located very close to the SNR sampling areas elevations ranging from 1894 m to 2910 m. Monthly mean temperature and monthly total precipitation both peaks in July (Fig. 1). Data from Lintao meteorological station are strongly correlated with those from the Linxia and Hezuo stations. Taking into account the regional representation and maximum correlation with the tree-ring chronology, only the climatic records from Lintao were used in the further analyses. Mean annual precipitation and mean annual air temperature of the Lintao station for the 57-year period (1951–2007) are 530 mm and 7.2 °C, respectively.

The two nearest (33.75°N, 103.75°E; 36.25°N, 103.75°E) monthly PDSI (Palmer, 1965) grid-point data (2.5° × 2.5°, Dai et al., 2004, 2011) were used to investigate the combined effects of precipitation, temperature and soil moisture on the SNR tree growth during the period 1951–2010. Positive and negative values of the PDSI correspond to wet and dry conditions, respectively. We also used the PDSI dataset to analyze moisture variability in monsoonal Asia during the period 1991–2000 in this paper.

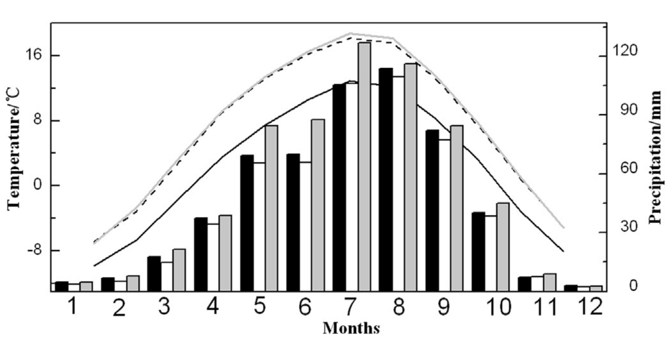

Fig. 1. Climate diagram for three meteorological stations in northern China. The gray and black lines and columns indicate temperature and precipitation at Hezuo and Linxia meteorological stations, respectively. The white columns and dashed line indicate precipitation and temperature at Lintao meteorological stations, respectively.

To study the regional moisture changes, we combined five moisture-sensitive tree ring-width series spanning the period 1804–1999 to extract the regional climate signals and discuss the regional climate mechanisms. Five tree-ring sites were selected in NCC along a belt running from northeast to southwest, as follows: Helan Mountains (Mts.; HL; Li et al., 2007), Hasi Mts. (HS; Kang et al., 2012), Xinglong Mts. (XL; Fang et al., 2009), Guiqing Mts. (GQ; Fang et al., 2010) and Songmingyan (this study). For the identification of common drought events, we used additional tree-ring sites located near NCC, namely the Kongtong Mts. (KT; Fang et al., 2012) and Changling Mts. (CL; Gao et al., 2006) chronologies, and a regional tree-ring record from the northeastern Tibetan Plateau (Yang et al., 2010).

To better understand regional climate variability, two moisture-related reconstruction datasets were used to analyze temporal and spatial variability. The DWI dataset published by the State Meteorological Administration (1981) mostly includes data from central and eastern China, which were derived from local historical documents, and are classified into five grades for each year: very wet (grade 1), wet (grade 2), normal (grade 3), dry (grade 4), very dry (grade 5). The DWI dataset can be adopted to analyze precipitation variability in eastern China for the last 500 years (Qian et al., 2012). We extracted 100 sites from the DWI dataset to analyze the moisture variation pattern in eastern China (east of 105°E) during the three drought periods recorded by tree-ring data from SNR.

The second dataset was the MADA (Cook et al., 2010) dataset, which is available at 2.5° by 2.5° resolution. It covers the past 700 years and was constructed by calibrating 327 tree-ring chronologies with 534 MADA grid points. This dataset has been used for studying spatial and temporal drought variations over the Tibetan Plateau and nearby regions (Wang et al., 2013; Yang et al., 2013b). However, the MADA dataset poorly represents drought variations in eastern China (Yang et al., 2013c). In this study, the MADA data were applied to investigate spatial and temporal patterns in the western region of monsoonal Asia (-20-60°N, 60-105°E), including a total of 347 MADA grid points. To facilitate comparison, these two datasets of DWI and MADA (hereafter MADA-DWI) were calculated to have consistent variation (for details, see Yang et al., 2013b). Positive values represent wetter conditions and negative values indicate dry conditions.

To investigate possible far-distant atmospheric influences on the moisture variability in NCC, the following data were also employed for further analysis: the PDO reconstruction (MacDonald and Case, 2005), PDO instrumental data (http://climexp.knmi.nl/) and AMO proxy (Gray et al., 2004).

2.2. Data analysis methods

Five single-site tree-ring chronologies (HL, HS, XL, GQ and Songmingyan) were subjected to a principal component analysis (Meeker and Mayewski, 2002; Yang et al., 2009) to identify the common signal of climate variations. The first PC expresses the strongest common component or the dominant similarity shared by the data and has broad scale spatial representation.

We processed the tree-ring data, AMO proxy and PDO index using a band-pass filter in the 50–70 year range.

2.3. The SNR chronology development

The SNR tree-ring data comprise 72 tree-ring cores extracted from 50 living trees in October 2010 at altitudes from 2540 to 2737 m a.s.l. To avoid the effects of tree competition within the tree population, the samples were taken from isolated living trees growing on steep slopes or cliffs. Wood cores were air dried and mounted on grooved sticks with the transverse surfaces facing up

(Phipps, 1985). Cores were prepared with razor blades to expose ring details at the cellular level (Stokes and Smiley, 1968). Ring widths were measured with a LINTAB 6 measuring system, at a precision of 0.01 mm. The tree-ring samples were cross-dated using the standard method in the software package TSAP-Win (Rinn, 2003). To confirm the exact dating for each ring-width series, the program COFECHA (Holmes, 1983) was used.

Ring-width chronologies were developed by the program ARSTAN (Cook, 1985). A data-adaptive power transformation was applied prior to standardization in order to remove bias caused by so-called heteroscedasticity (Cook and Peters, 1997). The biological trend inherent in the raw ring-width data series was removed by a negative exponential function, thereby retaining most low frequency variations.

From the three chronologies produced by the ARSTAN software, we selected the STD (standard chronology) version for further analysis (Fig. 2) since it contains considerable low-frequency variability related to long-term climate variations. After selecting the period with an expressed population signal (EPS) exceeding the threshold of 0.85 (Wigley et al., 1984), the confident part of the standard chronology covered the period AD 1804–2010. Fundamental descriptive statistics for the standard chronologies, like mean sensitivity (MS = 0.25) and signal-to-noise ratio (STNR = 44.7) indicate a strong common environmental forcing on the trees included in the standard chronology.

It is well-known that use this traditional technique to create a set of time series of tree-ring indices has unsettled statistical issues (Yang et al., 2012b). The essence of this critique is that traditional tree-ring-based paleoclimatic reconstructions are not capable to well reproduce longer-term (many-centennial) climate variations, and so the tree-ring processing technique has to be improved (Yang et al., 2014). However, since our tree-ring record is not long enough to study multi-century climate variability, our main goal is to analyze climate-induced variations of the tree growth on inter-decadal time scales only. Therefore, the application of traditional standardization technique is appropriate.

Correlation analyses (Fritts, 1976) between the ring-width series, monthly values of temperature and precipitation at the Lintao meteorological station, and with the two PDSI grid points (33.75°N, 103.75°E; 36.25°N, 103.75°E) were calculated with the DendroClim 2002 software (Biondi and Waikul, 2004). Climate-growth analyses were undertaken for the common period 1951–2008 for a time window starting from May of the previous year to October of the current year.

3. Results and discussion

3.1. Response to climate variables

Correlation analyses between the Songmingyan ring-width chronology and regional climate data revealed significant negative correlations ($p < 0.05$) with temperature in July and August of the previous year, and in February and June of the current year (Fig. 3). By contrast, there was a positive correlation between precipitation during the growing season and tree growth, which was particularly evident for July and August of the previous year and July of the current year. However, these correlation coefficients are not high, suggesting that neither temperature nor precipitation are dominant controlling factors for tree growth in the study area.

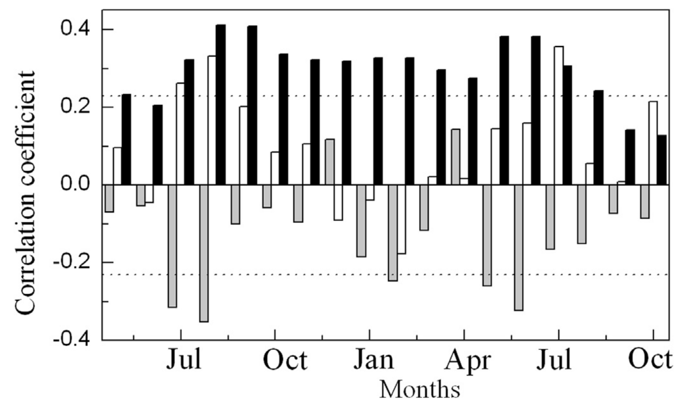

Fig. 3. Correlations between climate factors and Songmingyan standard chronology. Monthly correlations with mean temperature, total precipitation and PDSI are shown by gray, white and black bars, respectively. Horizontal dashed lines indicate the 95% confidence levels.

Therefore, we explored the correlation between ring-width and the monthly PDSI series over their common period of 1951–2010, thereby taking the combined effects of precipitation and temperature into account (Palmer, 1965). Ring-width showed higher correlations with the PDSI than both temperature and precipitation (Fig. 3), which is consistent with other tree-ring studies conducted in northern China (Fang et al., 2010; Kang et al., 2012; Li et al., 2007). Most of the correlations were significant at the 95% confidence level, except for those in September and October of the current year (Fig. 3). The highest correlation coefficient of the SNR tree-ring chronology were found with annual PDSI from previous August to current July ($r = 0.41$, $n = 60$, $p < 0.01$). The highest correlation coefficient between the SNA ring-width chronology and seasonal means of PDSI is 0.4 ($n = 60$, $p < 0.01$) for a season including current May to June. These correlations are relatively high, indicating that reduced tree growth in the study area was attributed to drought conditions.

3.2. Regional drought variability over the past 200 years

To test the regional representation of our tree-ring data, the SNR chronology was compared with other site and regional tree-ring

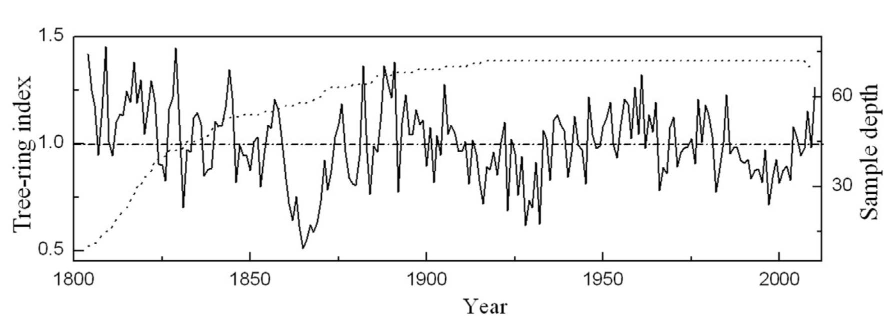

Fig. 2. Standard chronology for Songmingyan (black line) and sample size expressed as number of cores (dashed line).

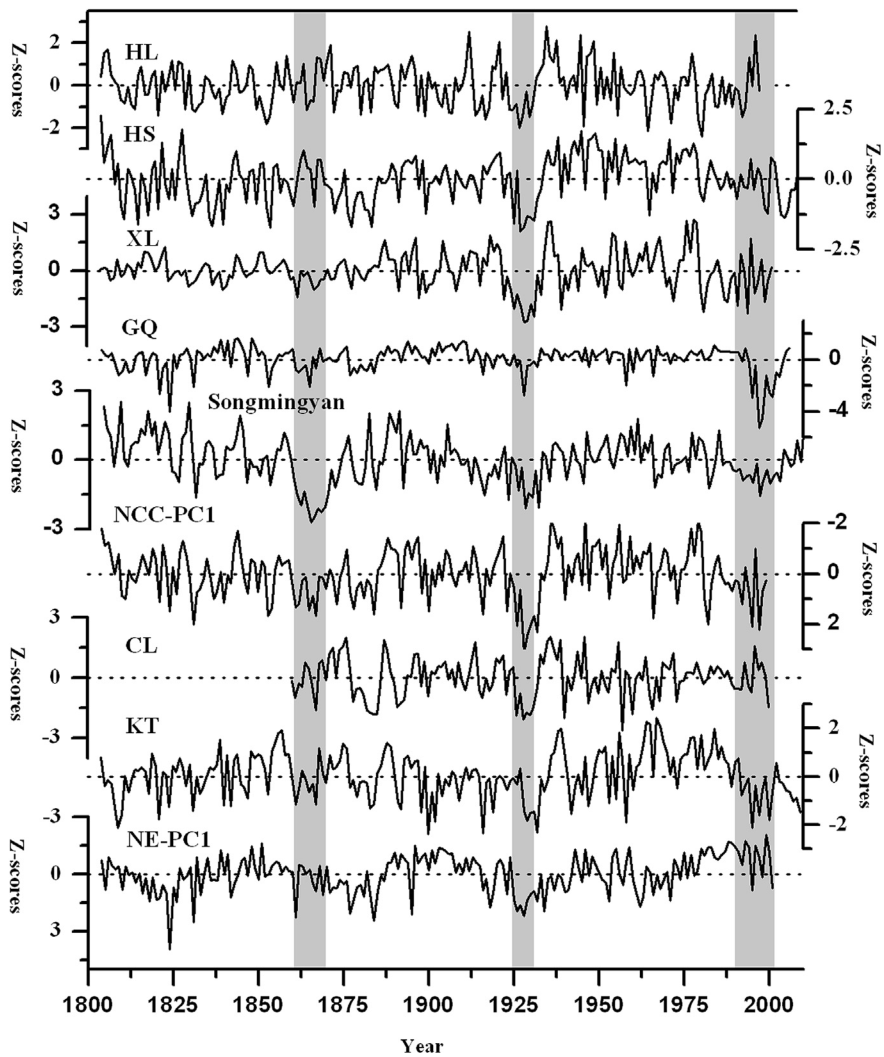

Fig. 4. Comparison between Songmingyan chronology and other climate reconstructions in NCC and the northeastern Tibetan Plateau. The shaded bars mark the severe drought periods of the 1860s, 1928–32, and 1991–2000. HL: Helan Mountains; HS: Hasi Mountains; XL: Xinglong Mountains; GQ: Guiqing Mountains; Songmingyan: this study; NCC-PC1: the first principal component of moisture variance in NCC; CL: Changling Mountains; KT: Kongtong Mountains; NE-PC1: the first principal component of moisture variance over the northeastern Tibetan Plateau. For a better comparison, the scales of NCC-PC1and NE-PC1 are inverted.

chronologies from NCC and the northeastern Tibetan Plateau (Fig. 4). These chronologies are located close to the northern fringe of the ASM. The chronology from CL was used as a precipitation reconstruction, and has a correlation coefficient with the Songmingyan chronology of 0.27 ($n = 141$). The PDSI reconstructions from KT are also significantly correlated with the Songmingyan ($r = 0.3$, $n = 206$). All these correlations are significant at the 0.01 level. Significant correlation ($r = -0.21$, $n = 197$) was also found between Songmingyan reconstruction and regional precipitation series over the northeastern Tibetan Plateau (Yang et al., 2010). In particular, the common minimum growth occurred during the 1860s, 1928–1932 and 1991–2000 in these chronologies, indicating that three common drought events occurred over a large spatial scale.

The HL, HS, XL and GQ series are all represent local PDSI reconstructions, and share similar drought variability with the Songmingyan chronology. It is important to mention that five chronologies (HL, HS, XL, GQ and Songmingyan) were produced using the same negative exponential or linear regression detrending methods which enhances comparability. Correlation analysis indicates strongly positive correlations among the five chronologies (Table 1).Thus, the dataset can be employed to analyze regional moisture variations in NCC. Principal component analysis was applied to the five tree-ring chronologies during the common period 1804–1999 to extract the common regional signal of climate variations. The first principal component of NCC (hereafter NCC-PC1) accounted for 49.3% of the total variance. The NCC-PC1 (negative) series showed strongly coherent variability with the other single-site records over the past 200 years (Fig. 4), especially

Table 1
Correlation matrix between five single-site tree-ring chronologies from NCC during the period 1804–1999.

	Helan Mts.	Hasi Mts.	Xinglong Mts.	Guiqing Mts.	Songmingyan
Helan Mts.	1				
Hasi Mts.	0.55	1			
Xinglong Mts.	0.39	0.46	1		
Guiqing Mts.	0.19	0.32	0.28	1	
Songmingyan	0.23	0.36	0.49	0.37	1

All correlations are significant at 99% confidence levels.

during drought periods. Therefore, the NCC-PC1 can be assumed to be a reliable indicator of moisture variations in NCC.

Regional drought characteristics were investigated by mapping spatial patterns of drought conditions during the extreme drought years of the 1860s, 1928–32 and 1991–2000 (Fig. 5). Fig. 5a, b and c were obtained using MADA-DWI dataset. Drought dominated over the central part of north China and Mongolia in the three periods of reduced tree-growth. During the period 1928–1932 (Fig. 5b), a severe drought occurred in the Indian subcontinent, whereas the western part of monsoonal Asia and Southeast Asia experienced wet conditions. Furthermore, Fig. 5c reveals an important phenomenon in which the drought in north China was enhanced in 1991–2000 and widely distributed across monsoonal Asia, including Southeast Asia, the Indian subcontinent, Kazakhstan and Mongolia. It is also noted that droughts occurred mainly in northern China, whereas the climate was relatively wet in southeast China. Similar results were obtained by Zhang et al. (1999).

The same pattern as that in Fig. 5c was found in Fig. 5d when we repeated the analysis using the instrumental PDSI (Dai et al., 2004) dataset from 1991 to 2000. The most severe drought was centered in north China, whereas wet conditions prevailed in northwest China. The study by Shi et al. (2003) also confirmed that the climate in northwest China, especially in the Xinjiang area, has shifted towards warm-wet conditions since 1987.

3.3. Multi-scale analysis of regional tree-ring records and their relationship to PDO

Based on the above analysis, the three episodes of reduced tree growth occurred quite regularly at 60 year recurrence intervals (see in Fig. 4). The length of the intervals corresponds to that of the atmospheric oscillation in the northern China climate system, showing 60–70 year cyclicity. This oscillation was first discovered in the North Atlantic climate (Schlesinger and Ramankutty, 1994). Sonechkin et al. (1999) assumed that this oscillation is a global phenomenon.

Previous studies found that the multi-decadal variations of AMO (Li and Gary, 2007) and PDO (MacDonald and Case, 2005) exhibit an oscillation with a typical period of 50–80 years. In order to explore relationships and possible linkage mechanisms between climate variability across NCC with AMO and PDO, 50–70 year band-pass filtering was performed during the common period. We calculated correlations between extracted waveforms of the AMO proxy and NCC-PC1 during the common period 1804–1990. The results suggested weak connection with the AMO ($r = 0.126$, $n = 187$). However, there are significant correlations with PDO.

Considering the stronger relationship with PDO, we focused on the influence of PDO on NCC moisture variability (Fig. 6). We found that there is a significant negative correlation between extracted

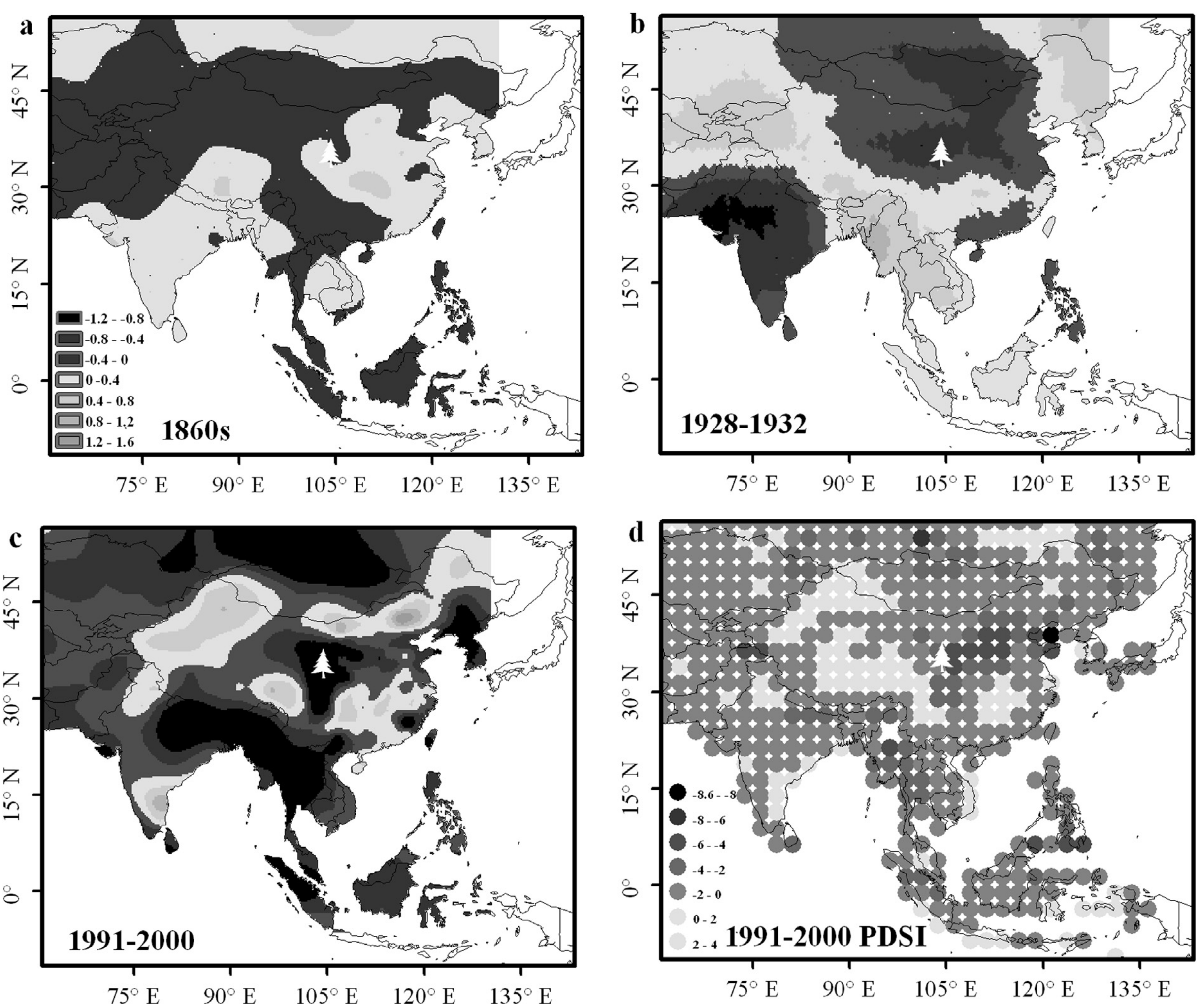

Fig. 5. Spatial patterns of droughts in the 1860s, 1928–32 and 1991–2000 across Asia. Black and gray colors indicate dry and wet conditions, respectively. The white tree symbol indicates the Songmingyan study site.

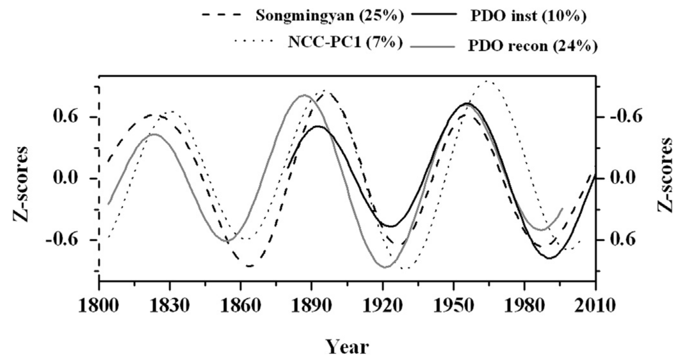

Fig. 6. Band-pass filtered time series in the range of periods 50–70 years for PDO instrumental (inst) data, PDO reconstruction (recon) data, the Songmingyan tree-ring index and PC1 series in NCC (NCC-PC1). The values in the brackets describe the variance in the band-pass filtered time series in relation to the corresponding unfiltered data series.

waveforms of the Songmingyan tree-ring index and PDO series. The correlation coefficients of the extracted waveforms of the Songmingyan chronology with the PDO reconstruction series and PDO instrumental series are −0.737 ($n = 193$, $p < 0.01$) and −0.916 ($n = 131$, $p < 0.01$), respectively. We also compared extracted waveforms of the negative NCC-PC1 with the PDO reconstruction series and PDO instrumental series. The resulting correlation coefficients are −0.842 ($n = 193$) and −0.882 ($n = 120$), respectively. The correlation is significant at the 0.01 level. There is an anti-phase relationship between the regional moisture variance and the PDO in cycle bands of 50–70 years. The PDO is in its warm phase when a negative sea surface temperature (SST) anomaly prevails in the North Pacific and a positive anomaly occurs in the central to eastern tropical Pacific. During boreal summer, the negative sea level pressure anomalies are much weaker in the North Pacific, while positive anomalies are enhanced over East Asia, as a result the East Asian summer monsoon is weakened. Consequently, northern China is much drier while the Yangtze River valley and southern, northeastern and northwestern China are wetter (Lu, 2005; Zhu and Yang, 2003). Therefore, the moisture regimes in NCC are linked to the multi-decadal variations of the PDO.

4. Conclusions

A new tree-ring chronology spanning the last 207 years was established in NCC to improve the existing tree ring network. It was found that the chronology showed stronger correlations with PDSI than with local temperature or precipitation. This revealed that our reconstruction represents drought variations within the study region. The driest epochs occurred during the 1860s, 1928–1932 and 1991–2000. Comparisons with other proxy record-based moisture reconstructions from nearby regions and the northeastern Tibetan Plateau suggest that the moisture variability across these marginal areas of monsoonal Asia shows similar frequencies and amplitudes, particularly during severe drought periods. Moreover, the spatial patterns of dry-wet conditions in Asia can be expressed very well by the MADA and DWI dataset. Large-scale extreme drought events strongly affected northern China and Mongolia during the three drought periods. The drought epoch during 1991–2000 was widely distributed across the Asian continent. The correlation analysis between PDO index and regional moisture variance at the 50–70 year time scale suggests that there were associations between dry epochs and the warm phases of PDO, supporting the hypothesis that PDO is a driving factor for multi-decadal variations of NCC drought. This multi-decadal oscillation represents a large-scale rather than a local phenomenon. Our conclusion has provided new insights into the past changes in moisture regimes which can improve quantification and understanding of the climate regime in NCC and might facility mitigation measures again regional drought events.

Acknowledgments

The authors extend many thanks to the editor Thanuj Chandran and two anonymous reviewers for their constructive comments. The study was supported by the National Natural Science Foundation of China (Grants #41325008), Interdisciplinary Innovation Team project of the CAS (29Y329B91), the CAS Visiting Professorship for Senior International Scientists (Grant No. 2010T1Z31) and Foundation for Excellent Youth Scholars of CAREERI (Y451061001), CAS. The authors are also grateful to Keyan Fang for providing relevant data.

References

Biondi, F., Waikul, K., 2004. DENDROCLIM2002: a C++ program for statistical calibration of climate signals in tree-ring chronologies. Comput. Geosci. 30, 303–311.
Chen, F., Yu, Z., Yang, M., Ito, E., Wang, S., Madsen, D.B., Huang, X., Zhao, Y., Sato, T., Birks, J., Boomer, I., Chen, J., An, C., Wünnemann, B., 2008. Holocene moisture evolution in arid central Asia and its out-of-phase relationship with Asian monsoon history. Quat. Sci. Rev. 27, 351–364.
Cook, E.R., 1985. A Time-series Analysis Approach to Tree-ring Standardization. Ph.D. Dissertation. The University of Arizona Press, Tucson.
Cook, E.R., Peters, K., 1997. Calculating unbiased tree-ring indices for the study of climatic and environmental change. Holocene 7, 361–370.
Cook, E.R., Anchukaitis, K.J., Buckley, B.M., D'Arrigo, R.D., Jacoby, G.C., Wright, W.E., 2010. Asian monsoon failure and megadrought during the last millennium. Science 328, 486–489.
Dai, A., 2011. Drought under global warming: a review. Wiley Interdiscip. Rev. Clim. Change 2, 45–65.
Dai, A.G., Trenberth, K.E., Qian, T., 2004. A global dataset of palmer drought severity index for 1870–2002: relationship with soil moisture and effects of surface warming. J. Hydrometeorol. 5, 1117–1130.
Fang, K.Y., Gou, X.H., Chen, F.H., Yang, M., Li, J., He, M., Zhang, Y., Tian, Q., Peng, J., 2009. Drought variations in the eastern part of Northwest China over the past two centuries: evidence from tree rings. Clim. Res. 38, 129–135.
Fang, K.Y., Gou, X.H., Chen, F.H., D'Arrigo, R., Li, J., 2010. Tree-ring based drought reconstruction for Guiqing Mountain (China): linkages to the Indian and Pacific Oceans. Int. J. Climatol. 30, 1137–1145.
Fang, K.Y., Gou, X.H., Chen, F.H., Liu, C.Z., Davi, N., Li, J.B., Zhao, Z.Q., Li, Y.J., 2012. Tree-ring based reconstruction of drought variability (1615–2009) in the Kongtong Mountain area, northern China. Global Planet. Change 80–81, 190–197.
Fritts, H.C., 1976. Tree Rings and Climate. Academic Press, London.
Gao, S.Y., Lu, R.J., Qiang, M.R., Hasi, E.R., Zhang, D.S., Chen, Y., Xiao, H., 2006. Reconstruction of precipitation in the last 140 years from tree ring at south margin of the Tengger Desert. Chin. Sci. Bull. 51, 326–331.
Gray, S.T., Graumlich, L.J., Betancourt, J.L., Pederson, G.T., 2004. A tree-ring based reconstruction of the Atlantic multidecadal oscillation since 1567 A.D. Geophys. Res. Lett. 31, L12205.
He, M.H., Yang, B., Datsenko, N.M., 2013. A six hundred-year annual minimum temperature history for the central Tibetan Plateau derived from tree-ring width series. Clim. Dyn. http://dx.doi.org/10.1007/s00382-013-1882-x.
Holmes, R.L., 1983. Computer-assisted quality control in tree-ring dating and measurement. Tree Ring Bull. 43, 69–95.
Kang, S.Y., Yang, B., Qin, C., 2012. Recent tree-growth reduction in north central China as a combined result of a weakened monsoon and atmospheric oscillations. Clim. Change 115, 519–536.
Li, S.L., Gary, B.T., 2007. Influence of the Atlantic multidecadal oscillation on the winter climate of East China. Adv. Atmos. Sci. 24, 126–135.
Li, J., Chen, F., Cook, E.R., Gou, X.H., Zhang, Y., 2007. Drought reconstruction for north central China from tree rings: the value of the Palmer drought severity index. Int. J. Climatol. 27, 903–909.
Lu, R.Y., 2005. Interannual variation of North China rainfall in rainy season and SSTs in the equatorial eastern Pacific. Chin. Sci. Bull. 50, 2069–2073.
Ma, Z.G., 2007. The interdecadal trend and shift of dry/wet over the central part of North China and their relationship to the Pacific Decadal Oscillation (PDO). Chin. Sci. Bull. 52, 2130–2139.
MacDonald, G.M., Case, R.A., 2005. Variations in the Pacific Decadal Oscillation over the past millennium. Geophys. Res. Lett. 32, L08703.
Meeker, L.D., Mayewski, P.A., 2002. A 1400 year long record of atmospheric circulation over the North Atlantic and Asia. Holocene 12, 257–266.
Palmer, W.C., 1965. Meteorological Drought. Weather Bureau Research Paper 45. US Department of Commerce, Washington, DC.

Phipps, R.L., 1985. Collecting, Preparing, Crossdating, and Measuring Tree Increment Cores. Water-resources Investigations Report. US Geological Survey, Denver CO, pp. 85–4148.
Qian, W., Shan, X., Chen, D., Zhu, C., Zhu, Y., 2012. Droughts near the northern fringe of the East Asian summer monsoon in China during 1470-2003. Clim. Change 110, 373–383.
Qin, C., Yang, B., Bräuning, A., Sonechkin, D.M., Huang, K., 2010. Regional extreme climate events on the northeastern Tibetan Plateau since AD 1450 inferred from tree rings. Global Planet Change 75, 143–154.
Qin, C., Yang, B., Melvin, T.M., Fan, Z., Zhao, Y., Keith, R.B., 2013. Radial growth of Qilian Juniper on the northeast tibetan plateau and Potential climate associations. PLoS ONE 8, e79362.
Rinn, F., 2003. TSAP-win: Time Series Analysis and Presentation for Dendrochronology and Related Applications. Version 0.55 User Reference. Heidelberg, Germany. http://www.rimatech.com.
Schlesinger, M.E., Ramankutty, N., 1994. An oscillation in the global climate system of period 65-70 years. Nature 367, 723–726.
Shao, X.M., Wan, S.Z., Xu, Y., Zhu, H.F., Xu, X.G., Xiao, Y.M., 2007. A 3500-year master tree-ring dating chronology from the northeastern part of the Qaidam Basin. Quat. Sci. 27, 477–485.
Shi, Y.F., Shen, Y.P., Kang, E.S., Li, D.L., Ding, Y.J., Zhang, G.W., Hu, R.J., 2003. Recent and future climate change in northwest China. Clim. Change 80, 379–393.
Sonechkin, D.M., Astafyeva, N.M., Datsenko, N.M., Ivachtchenko, N.N., Jakubiak, B., 1999. Multiscale oscillations of the global climate system as revealed by wavelet transform of observational data time series. Appl. Theor. Climatol. 64, 131–142.
Song, H.M., Liu, Y., 2011. PDSI variations at Kongtong Mountain, China, inferred from a 283-year *Pinus tabulaeformis* ring width chronology. J. Geophys. Res. 116, D22111.
State Meteorological Administration, 1981. Yearly Charts of Dryness/wetness in China for the Last 500-year Period. China Map Press, Beijing.
Stokes, M.A., Smiley, T.L., 1968. An Introduction to Tree-ring Dating. The University of Chicago Press, Chicago, London.
Wang, J.L., Yang, B., Qin, C., Kang, S.Y., 2013. Spatial patterns of moisture variations across the Tibetan Plateau during the past 700 years and their relationship with atmospheric oscillation modes. Int. J. Climatol. http://dx.doi.org/10.1002/joc.3715.
Wigley, T., Briffa, K.R., Jones, P.D., 1984. On the average value of correlated time series, with applications in dendroclimatology and hydrometeorology. J. Appl. Meteorol. 23, 201e213.
Yang, B., Wang, J.S., Bräuning, A., Dong, Z.B., Esper, J., 2009. Late Holocene climatic and environmental changes in arid central Asia. Quat. Int. 194, 68–78.
Yang, B., Qin, C., Huang, K., Fan, Z.X., Liu, J.J., 2010. Spatial and temporal patterns of variations in tree growth over the northeastern Tibetan Plateau during the period AD 1450-2001. Holocene 20, 1235–1245.
Yang, B., Qin, C., Shi, F., Sonechkin, D.M., 2012a. Tree ring-based annual streamflow reconstruction for the Heihe River of arid northwestern China since AD 575 and its implication to water resources management. Holocene 22, 773–784.
Yang, B., Sonechkin, D.M., Datsenko, N.M., Ivashchenko, N.N., Liu, J.J., Qin, C., 2012b. The eigen analysis of tree-ring records: Part 2, Posing the eigen problem. Theor. Appl. Climatol. 107, 131–141.
Yang, B., Sonechkin, D.M., Datsenko, N.M., Ivashchenko, N.N., Liu, J.J., Qin, C., 2012c. The eigen analysis of tree-ring records: Part 3, taking heteroscedasticity and sampling effects into consideration. Theor. Appl. Climatol. 107, 519–530.
Yang, B., He, M.H., Melvin, T.M., Zhao, Y., Briffa, K.R., 2013a. Climate control on tree growth at the Upper and lower Treelines: a case study in the Qilian mountains, tibetan plateau. PLoS ONE 8, e69065.
Yang, B., Kang, S.Y., Fredrik, C.L., He, M.H., Zhao, Y., Qin, C., 2013b. Drought variability at the northern fringe of the Asian summer monsoon region over the past millennia. Clim. Dyn. http://dx.doi.org/10.1007/s00382-013-1962-y.
Yang, F.M., Shi, F., Kang, S.Y., Wang, S., Xiao, Z., Nakatsuka, T., Shi, J., 2013c. Comparison of the dryness/wetness index in China with the Monsoon Asia Drought Atlas. Theor. Appl. Climatol. 114, 553–566.
Yang, B., Qin, C., Wang, J.L., He, M.H., Melvin, T.M., Osborn, T.J., Briffa, K.R., 2014. A 3,500-year tree-ring record of annual precipitation on the northeastern Tibetan Plateau. PNAS 111, 2903–2908.
Zhang, R., Sumi, A., Kimoto, M., 1999. A diagnostic study of the impact of El Niño on the precipitation in China. Adv. Atmos. Sci. 16, 229–241.
Zhu, Y.M., Yang, X.Q., 2003. Relationships between pacific decadal oscillation (PDO) and climate variabilities in China. Acta Meteorol. Sin. 61, 641–665.